

# Cytosolic phospholipase A<sub>2</sub> regulates viability of irradiated vascular endothelium

EM Yazlovitskaya<sup>1,2</sup>, AG Linkous<sup>1</sup>, DK Thotala<sup>1</sup>, KC Cuneo<sup>1</sup> and DE Hallahan<sup>\*,1,2,3</sup>

Radiosensitivity of various normal tissues is largely dependent on radiation-triggered signal transduction pathways. Radiation simultaneously initiates distinct signaling from both DNA damage and cell membrane. Specifically, DNA strand breaks initiate cell-cycle delay, strand-break repair or programmed cell death, whereas membrane-derived signaling through phosphatidylinositol 3-kinase/Akt and mitogen-activated protein kinase/extracellular signal-regulated kinase (ERK) enhances cell viability. Here, activation of cytosolic phospholipase A<sub>2</sub> (cPLA<sub>2</sub>) and production of the lipid second-messenger lysophosphatidylcholine were identified as initial events (within 2 min) required for radiation-induced activation of Akt and ERK1/2 in vascular endothelial cells. Inhibition of cPLA<sub>2</sub> significantly enhanced radiation-induced cytotoxicity due to an increased number of multinucleated giant cells and cell cycle-independent accumulation of cyclin B1 within 24–48 h of irradiation. Delayed programmed cell death was detected at 72–96 h after treatment. Endothelial functions were also affected by inhibition of cPLA<sub>2</sub> during irradiation resulting in attenuated cell migration and tubule formation. The role of cPLA<sub>2</sub> in the regulation of radiation-induced activation of Akt and ERK1/2 and cell viability was confirmed using human umbilical vein endothelial cells transfected with shRNA for cPLA<sub>2</sub>α and cultured embryonic fibroblasts from cPLA<sub>2</sub>α<sup>-/-</sup> mice. In summary, an immediate radiation-induced cPLA<sub>2</sub>-dependent signaling was identified that regulates cell viability and, therefore, represents one of the key regulators of radioresistance of vascular endothelial cells.

*Cell Death and Differentiation* (2008) 15, 1641–1653; doi:10.1038/cdd.2008.93; published online 20 June 2008

The immediate molecular events that trigger the biological response to ionizing radiation are initiated by the hydrolysis of water. The resulting hydroxyl radicals interact with cellular components such as DNA resulting in DNA strand breaks and subsequent activation of well-described signal transduction pathways. In contrast, immediate signal transduction initiated at the cell membrane is less well characterized. For example, ceramide is generated in endothelial cells within minutes after exposure to 20 Gy radiation that later results in apoptosis.<sup>1,2</sup> However, endothelial cell viability is not affected by low doses of radiation (2–5 Gy) pointing to involvement of the activation of pro-survival phosphatidylinositol 3-kinase (PI3K)/Akt signaling.<sup>3–6</sup>

There is a growing number of reports demonstrating increased viability of vascular endothelial cells in response to low doses of ionizing radiation due to activation of pro-survival signaling pathways.<sup>5–9</sup> Biologically active lipids and proteins, such as phospholipases, lipid kinases, and phosphatases, which regulate the production of lipid second messengers, can initiate pro-survival signal transduction.<sup>10,11</sup> For example, phospholipase A<sub>2</sub> (PLA<sub>2</sub>) hydrolyzes phospholipids at the *sn*-2-acyl ester bond, generating free fatty acids and lysophospholipid second messengers.<sup>12</sup> The PLA<sub>2</sub>

superfamily can be divided into 10 enzyme groups by gene sequences. On the basis of biological properties, the classification of PLA<sub>2</sub> can be simplified into three main types: the cytosolic (cPLA<sub>2</sub>), the secretory (sPLA<sub>2</sub>), and the intracellular Ca<sup>2+</sup>-independent (iPLA<sub>2</sub>).<sup>12</sup> In mammalian cells, the *sn*-2-position of phospholipids is enriched with arachidonic acid (AA).<sup>13</sup> On the other hand, the most abundant phospholipid in mammalian cell membranes is phosphatidylcholine. Therefore, in addition to the release of free AA, the activation of cPLA<sub>2</sub> increases production of lysophosphatidylcholine (LPC).

LPC functions as the second messenger in signal transduction pathways, that regulate a number of cellular responses.<sup>12,14</sup> Recent publications suggest an important role of LPC in endothelial cell activation leading to increased vascular proliferation, migration, expression of adhesion molecules, and inflammation. LPC stimulated proliferation in endothelial cells by transactivating the vascular endothelial growth factor receptor 2 and activating Akt and extracellular signal-regulated kinase (ERK)1/2.<sup>15</sup> Increased levels of LPC are linked directly to cytokine and chemokine production in endothelial cells by activating mitogen-activated protein kinase (MAPK) and PI3K/Akt pathways, thus regulating the

<sup>1</sup>Department of Radiation Oncology, Vanderbilt University School of Medicine, Vanderbilt University, Nashville, TN, USA; <sup>2</sup>Vanderbilt-Ingram Cancer Center, Vanderbilt University School of Medicine, Vanderbilt University, Nashville, TN, USA and <sup>3</sup>Department of Cancer Biology, Vanderbilt University School of Medicine, Vanderbilt University, Nashville, TN, USA

\*Corresponding author: DE Hallahan, Department of Radiation Oncology, Vanderbilt University School of Medicine, Vanderbilt University, 1301 22nd Avenue South, B-902 The Vanderbilt Clinic, Nashville, TN 37232-5671, USA. Tel: + 615 343 9244; Fax: + 615 343 3075; E-mail: dennis.hallahan@vanderbilt.edu

**Keywords:** vascular endothelium; ionizing radiation; cytosolic phospholipase A<sub>2</sub>; apoptosis; lipid signal transduction

**Abbreviations:** PLA<sub>2</sub>, phospholipase A<sub>2</sub>; PI3K, phosphatidylinositol 3-kinase; MAPK, mitogen-activated protein kinase; ERK, extracellular signal-regulated kinase; AA, arachidonic acid; LPC, lysophosphatidylcholine; HUVECs, human umbilical vein endothelial cells; MEFs, mouse embryonic fibroblasts; PBS, phosphate-buffered saline; TLC, thin-layer chromatography; PI, propidium iodide; DAPI, 4',6-diamidino-2-phenylindole

Received 03.12.07; revised 19.5.08; accepted 26.5.08; Edited by SH Kaufmann Cio; published online 20.6.08

chemotaxis of particular leukocyte subpopulations during inflammation.<sup>16</sup> LPC also displays biphasic regulation of inflammatory factors in endothelial cells, causing activation of NF- $\kappa$ B at low concentrations and its inhibition at higher concentrations.<sup>17</sup>

Pro-survival signal transduction activated by ionizing radiation within vascular endothelium includes PI3K/Akt (PI3K/Akt) and MAPK pathways.<sup>4,6,7,9,18</sup> These pathways determine cellular response and sensitivity to radiation by ultimately controlling cell metabolism, proliferation, and cell death.<sup>7,19</sup> In the present study, we identified a sequence of molecular events in irradiated vascular endothelial cells, constituting an immediate pro-survival signaling pathway activated by ionizing radiation. This pathway involves activation of cPLA<sub>2</sub> followed by the increased production of LPC, transactivation of Flk-1 and phosphorylation of Akt and ERK1/2. This pathway can contribute to endothelial cell viability.

## Results

**Temporal relationship of Akt and ERK1/2 phosphorylation and activation of cytosolic PLA<sub>2</sub> following 3 Gy radiation.** We have previously reported radiation-induced phosphorylation of Akt in endothelial cells.<sup>5,6</sup> Comparison of treated cells with a time-matched sham-irradiated control demonstrated that maximal phosphorylation of Akt, as well as ERK1/2, occurred at 3 min after irradiation with 3 Gy (Figures 1a and b). Increased Akt phosphorylation at Thr<sup>308</sup>/Ser<sup>473</sup> was first detected at 2 min after exposure to 3 Gy radiation (1.8-fold increase over sham-irradiated control; Figure 1b), reached maximum after 3 min (2.4-fold increase), and remained elevated at 10 min (1.3-fold increase). ERK1/2 phosphorylation at Thr<sup>202</sup>/Tyr<sup>204</sup> in response to treatment with 3 Gy radiation was transient, first noticed as early as 2 min after the beginning of irradiation (1.3-fold increase), reaching maximum at 3 min (1.73-fold increase), and returning to basal level at 10 min (Figure 1b). Total cellular PLA<sub>2</sub> was activated during a similar time course (Figure 1c). The maximal activation of PLA<sub>2</sub> occurred 3 min after irradiation (3.36-fold increase over sham-irradiated control; Figure 1c), which coincided with the peak phosphorylation of ERK1/2 and Akt (Figures 1a–c). To determine which of the subtypes of the PLA<sub>2</sub> family is activated by 3 Gy radiation, we treated human umbilical vein endothelial cells (HUVECs) with specific inhibitors of cPLA<sub>2</sub> (1  $\mu$ M AACOCF<sub>3</sub> or 1  $\mu$ M methyl arachidonyl fluorophosphonate, MAFP), sPLA<sub>2</sub> (100 nM sPLA<sub>2</sub>-IIA inhibitor I) or iPLA<sub>2</sub> (1  $\mu$ M PACOCF<sub>3</sub>) for 30 min prior to exposure to 3 Gy radiation. The concentrations of inhibitors that were used in experiments were chosen to assure the specific effects for the subtypes of the PLA<sub>2</sub> family. AACOCF<sub>3</sub> is a potent and selective slow-binding inhibitor of cytosolic PLA<sub>2</sub> (IC<sub>50</sub> = 2–10  $\mu$ M for various cells); MAFP is irreversible inhibitor of both calcium-dependent and -independent cytosolic PLA<sub>2</sub> (IC<sub>50</sub> = ~2 and 5  $\mu$ M for cPLA<sub>2</sub> and iPLA<sub>2</sub>, respectively); sPLA<sub>2</sub>-IIA inhibitor I was shown to effectively block sPLA<sub>2</sub>-IIA-induced PGE<sub>2</sub> production at 100 nM in human rheumatoid synoviocytes; PACOCF<sub>3</sub> is novel Ca<sup>2+</sup>-independent PLA<sub>2</sub> inhibitor

with IC<sub>50</sub> = 3.8  $\mu$ M (for references see <http://www.emdbiosciences.com>). Cells were harvested 3 min after the beginning of irradiation. In HUVECs pretreated with inhibitors of cPLA<sub>2</sub>, radiation-induced activation of PLA<sub>2</sub> was completely abrogated (Figure 1d). In comparison, pretreatment of cells with inhibitors of sPLA<sub>2</sub> or iPLA<sub>2</sub> showed less than 20% decrease in PLA<sub>2</sub> activation (Figure 1d). These data suggest that the major PLA<sub>2</sub> subtype activated by low dose of ionizing radiation is the cytosolic isoform, cPLA<sub>2</sub>. To determine whether cPLA<sub>2</sub> participates in radiation-induced phosphorylation of ERK1/2 and Akt, HUVECs were pretreated with the inhibitors for cPLA<sub>2</sub>, sPLA<sub>2</sub>, or iPLA<sub>2</sub>, irradiated with 3 Gy and lysed at 3 min after irradiation. Western blot analysis showed that inhibitors of cPLA<sub>2</sub>, but not the inhibitors of sPLA<sub>2</sub> or iPLA<sub>2</sub>, markedly decreased radiation-induced activation of Akt and ERK1/2, suggesting that cPLA<sub>2</sub> contributes to the radiation-induced activation of these kinases (Figures 1e and f).

To verify the role of cPLA<sub>2</sub>, we studied radiation-induced phosphorylation of Akt and ERK1/2 in HUVECs that were transiently transfected with nonsilencing shRNA or shRNA for the predominant isoform of the enzyme cPLA<sub>2 $\alpha$</sub> , and mouse embryonic fibroblasts (MEFs) from knockout (KO) mice for cPLA<sub>2 $\alpha$</sub>  (cPLA<sub>2 $\alpha$</sub> <sup>-/-</sup>) and wild-type mice (cPLA<sub>2 $\alpha$</sub> <sup>+/+</sup>).<sup>13</sup> Transient transfection of HUVECs with cPLA<sub>2 $\alpha$</sub> -shRNA leads to an ~70% decrease in cPLA<sub>2 $\alpha$</sub>  protein level compared to nonsilencing shRNA (Figure 2a). Irradiation of HUVECs transfected with nonsilencing shRNA resulted in time course of Akt and ERK1/2 phosphorylation similar to that observed in irradiated nontransfected HUVECs (Figures 2b and 1a). A similar trend, but with less pronounced activation was observed in irradiated MEF<sup>cPLA<sub>2 $\alpha$</sub> +/+</sup> (Figure 2c). Radiation-induced phosphorylation of Akt and ERK1/2 was completely abrogated in HUVECs transfected with cPLA<sub>2 $\alpha$</sub> -shRNA (Figure 2b) as well as in MEF<sup>cPLA<sub>2 $\alpha$</sub> -/-</sup> (Figure 2c) resembling the effect of cPLA<sub>2 $\alpha$</sub>  inhibitors (Figures 1e and f). These genetic knockdown and KO models support the regulatory role of cPLA<sub>2</sub> and implicate involvement of its  $\alpha$ -isoform in radiation-induced activation of pro-survival kinases Akt and ERK1/2.

**Radiation-induced LPC production and effects of exogenously added LPC species.** As the most abundant phospholipid in the mammalian cell membrane is phosphatidylcholine, radiation-induced activation of cPLA<sub>2</sub> could lead to the increased production of LPC. To determine whether 3 Gy radiation induces LPC production, we labeled HUVECs with <sup>3</sup>H-palmitic acid for 90 min and then treated with 3 Gy. Thin-layer chromatography (TLC) of extracted total lipids from the irradiated HUVECs revealed a statistically significant increase in LPC production of 1.6-fold compared to untreated cells (Figures 3a and b). To determine whether this increase in LPC is involved in radiation-induced signal transduction, we compared HUVEC response to ionizing radiation to the response triggered by various exogenously added LPC species. Four different LPC species (up to 20  $\mu$ M) led to a slight increase in cell proliferation (up to 20%; Figure 3c). Following this observation, we studied the effect of LPC on the activation of pro-survival pathways. Four LPC species (10  $\mu$ M) added to HUVECs resulted in ERK1/2 and

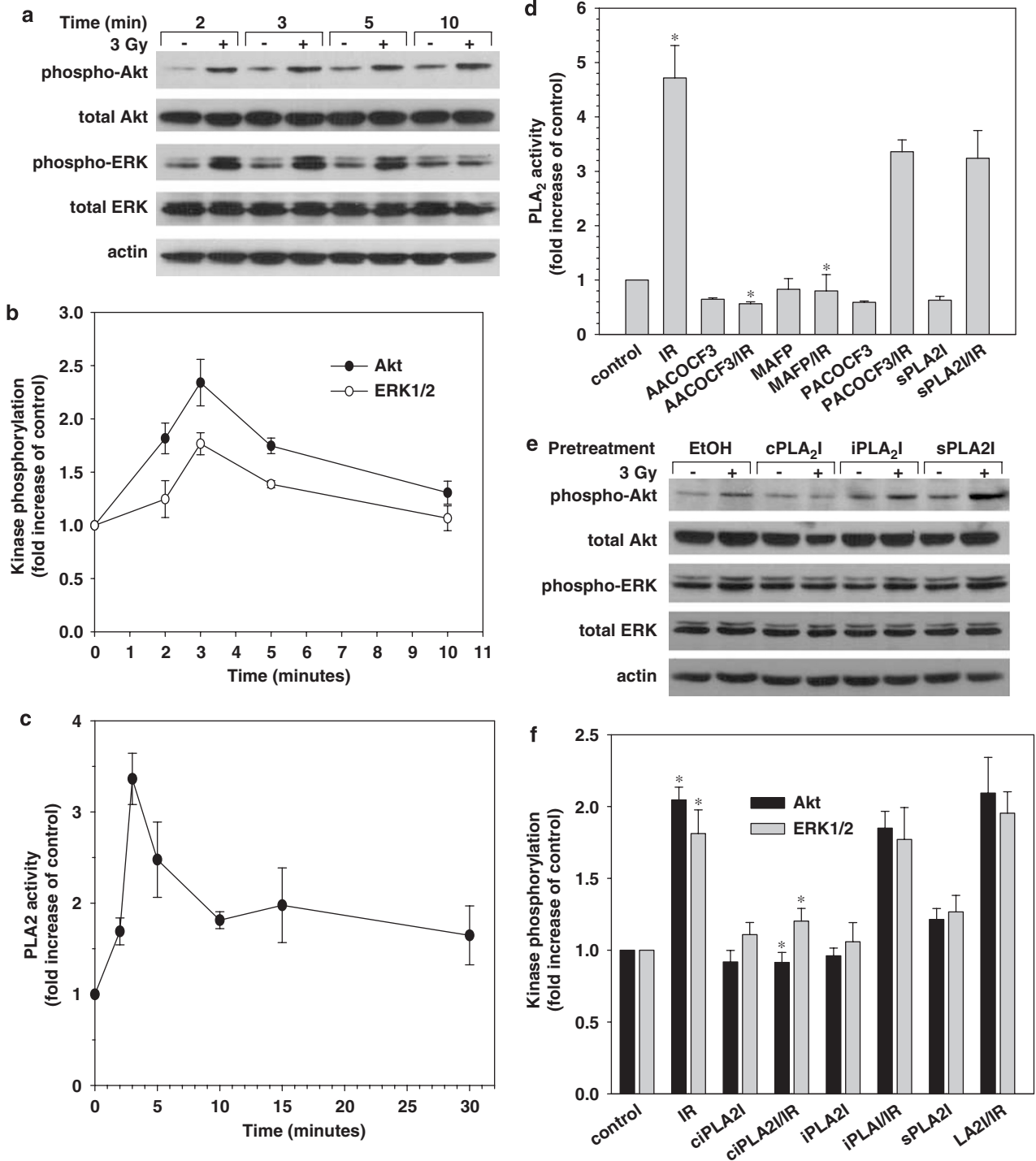


**Figure 1** Cytosolic phospholipase A<sub>2</sub> (cPLA<sub>2</sub>) is required for radiation-induced extracellular signal-regulated kinase (ERK)1/2 and Akt phosphorylation in irradiated human umbilical vein endothelial cells (HUVECs). (a–c) HUVECs were treated with 3 Gy and lysed 2–30 min after the beginning of irradiation. (a) Western blot analysis with phospho-specific antibodies to Akt<sup>Thr308/Ser473</sup> or ERK1/2<sup>Thr202/Tyr204</sup>, total Akt or ERK1/2, and actin is shown. (b) The densitometry of Akt and ERK1/2 phosphorylation and S.E.M. from four experiments is shown. (c) The enzymatic activity of PLA<sub>2</sub> and S.E.M. from three experiments is shown. (d–f) HUVECs were treated with 3 Gy radiation or in combination with PLA<sub>2</sub> inhibitors 1 μM AACOCF<sub>3</sub>; 1 μM MAFP (methyl arachidonyl fluorophosphonate), cPLA<sub>2</sub> inhibitors; 1 μM PACOCF<sub>3</sub>, intracellular Ca<sup>2+</sup>-independent phospholipase A<sub>2</sub> (iPLA<sub>2</sub>) inhibitor; and 100 nM secretory phospholipase A<sub>2</sub> (sPLA<sub>2</sub>) inhibitor, which were added 30 min before irradiation. Cells were lysed 3 min after the beginning of irradiation. (d) The enzymatic activity of PLA<sub>2</sub> and S.E.M. from three experiments is shown; \**P* < 0.05. (e) The western blot for phospho-Akt, phospho-ERK1/2, total Akt or ERK1/2, and actin is shown. (f) The densitometry of Akt and ERK1/2 phosphorylation and S.E.M. from four experiments is shown

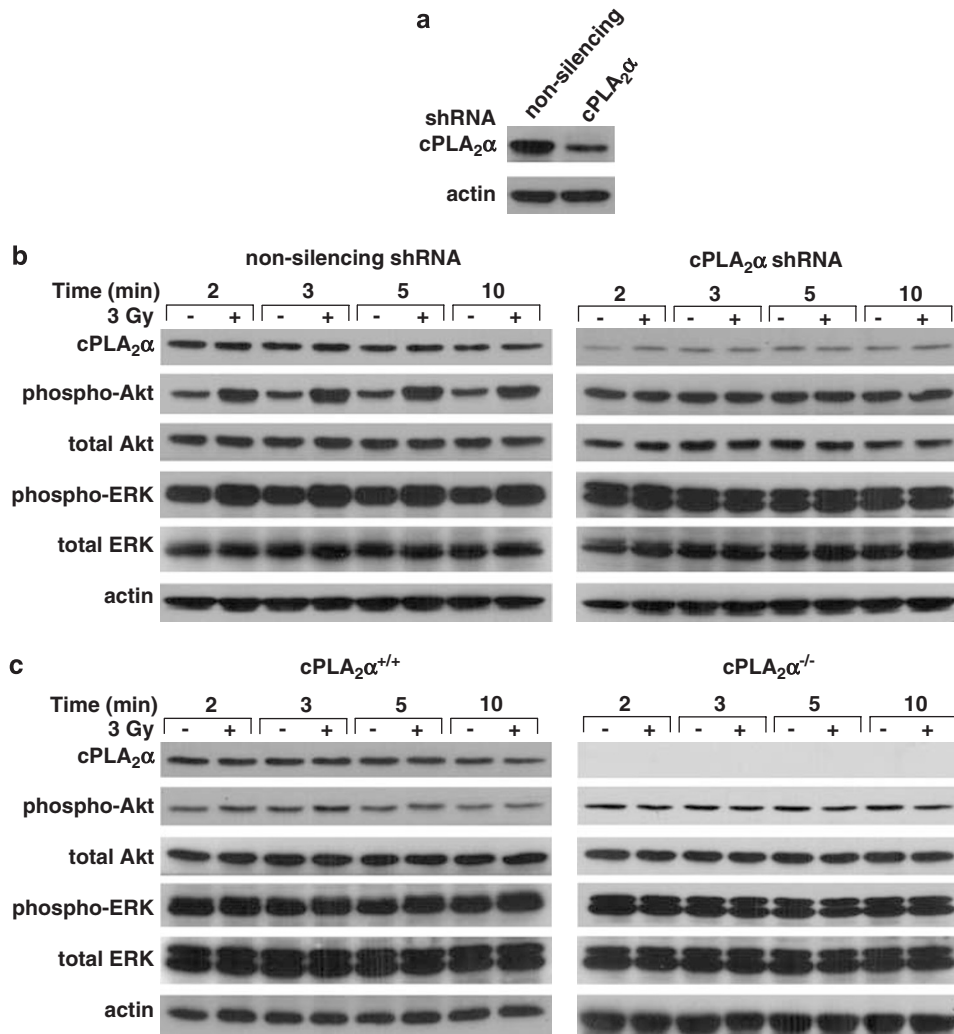


**Figure 2** Knockout or knockdown of cytosolic phospholipase A<sub>2</sub> (cPLA<sub>2</sub>) $\alpha$  prevents radiation-induced extracellular signal-regulated kinase (ERK)1/2 and Akt phosphorylation in irradiated cells. (a, b) Human umbilical vein endothelial cells (HUVECs) were transiently transfected with nonsilencing shRNA or shRNA for cPLA<sub>2</sub> $\alpha$ , treated with 3 Gy radiation and lysed 2–10 min after the beginning of irradiation. The western blot analysis for cPLA<sub>2</sub> $\alpha$ , phospho-Akt, phospho-ERK1/2, total Akt or ERK1/2, and actin is shown. (c) Embryonic fibroblasts from mice with wild-type cPLA<sub>2</sub> $\alpha$  (cPLA<sub>2</sub> $\alpha$ <sup>+/+</sup>) and from cPLA<sub>2</sub> $\alpha$  KO mice (cPLA<sub>2</sub> $\alpha$ <sup>-/-</sup>) were treated with 3 Gy and lysed 2–10 min after the beginning of irradiation. The western blot for cPLA<sub>2</sub> $\alpha$ , phospho-Akt, phospho-ERK1/2, total Akt or ERK1/2, and actin is shown

Akt phosphorylation with the maximum phosphorylation at 5 min (Figures 3d and e). This maximal phosphorylation time point correlates with the time course of radiation-induced activation of ERK1/2 and Akt (Figures 1a and b).

**Radiation-induced activation of Flk-1.** As Flk-1 has recently been reported to be transactivated by LPC in HUVECs,<sup>15</sup> we studied activation of Flk-1 in radiation-induced signaling as a possible connection between increased production of LPC and phosphorylation of ERK1/2 and Akt. HUVECs were irradiated with 3 Gy, lysed 3–30 min later and subjected to western blot analysis. Treatment with 10 ng/ml VEGF for 15 min was used as a positive control. In response to 3 Gy radiation, phosphorylation of Flk-1 at Tyr<sup>951</sup> was increased as early as 3 min after treatment, whereas two other activating phosphorylation sites, Tyr<sup>1175</sup> and Tyr<sup>1212</sup>, were not affected (Figure 4a). This phosphorylation was transient and correlated well with time course of activation of

ERK1/2 and Akt (Figures 1a and b). To determine whether cPLA<sub>2</sub> participates in radiation-induced phosphorylation of Flk-1, HUVECs were treated with the cPLA<sub>2</sub>, sPLA<sub>2</sub>, or iPLA<sub>2</sub> inhibitors 30 min prior to radiation with 3 Gy. Western blot analysis showed that only cPLA<sub>2</sub> inhibition prevented radiation-induced phosphorylation of Flk-1 at Tyr<sup>951</sup> (Figure 4b).

**Involvement of cPLA<sub>2</sub> in radiation-induced cell death.** To determine the role of cPLA<sub>2</sub> in the viability of irradiated endothelial cells, we used specific cPLA<sub>2</sub> inhibitors in a number of cell survival assays. Clonogenic survival analysis showed that each inhibitor produced a statistically significant decrease in viability of HUVECs compared to irradiation alone (Figure 5a). This effect was specific for cPLA<sub>2</sub> inhibitors and was not observed when inhibitors for Ca<sup>2+</sup>-independent or secretory PLA<sub>2</sub> were used (Figure 5b). To determine the molecular mechanisms of

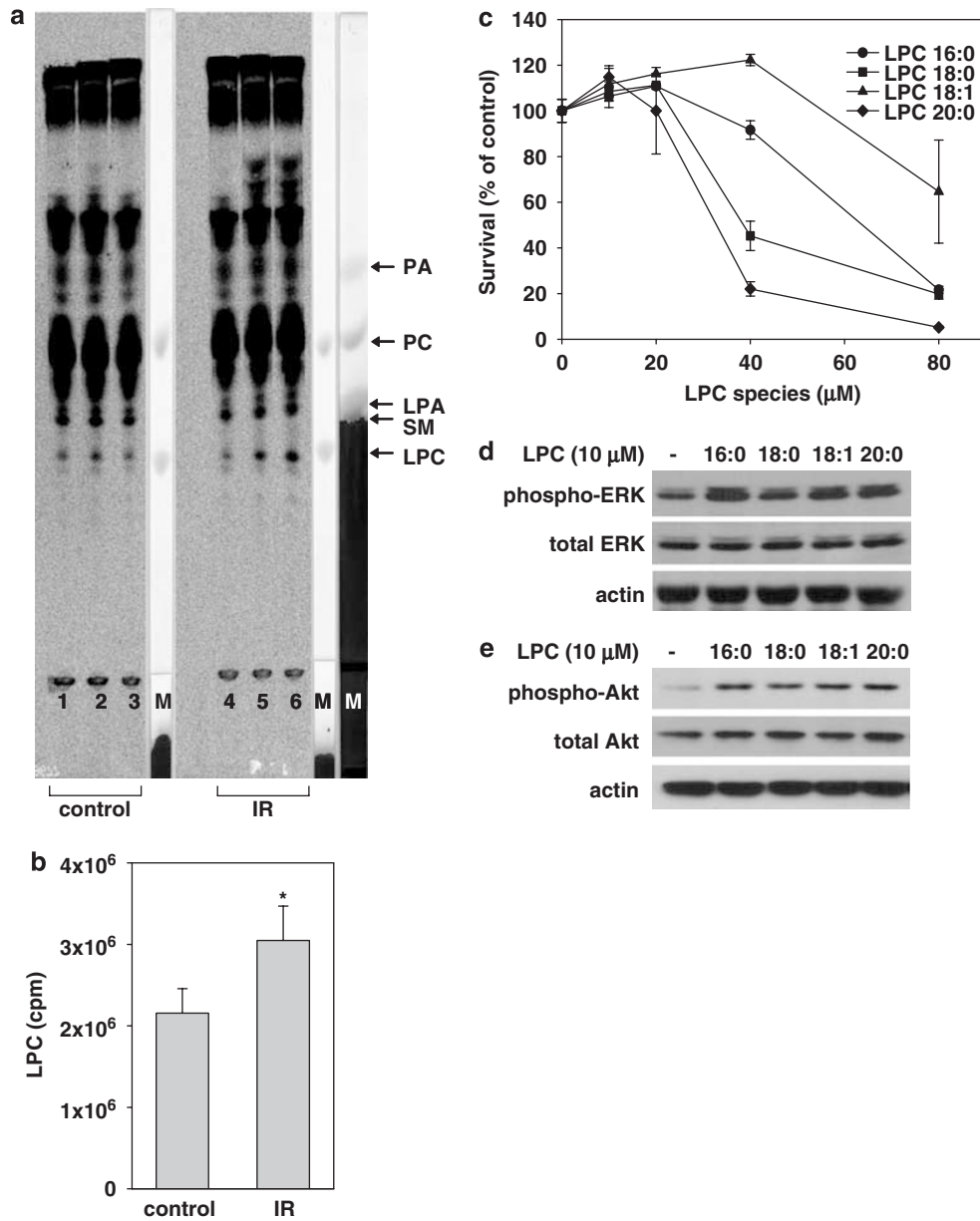


**Figure 3** Radiation induces increased lysophosphatidylcholine (LPC) production that leads to phosphorylation of extracellular signal-regulated kinase (ERK)1/2 and Akt. (a, b) Human umbilical vein endothelial cells (HUVECs) were labeled with <sup>3</sup>H-palmitic acid for 90 min and irradiated with 3 Gy. Total cellular phospholipids were extracted 3 min after irradiation. (a) Thin-layer chromatography (TLC) of extracted and standard lipids is shown. (b) A bar graph of quantification of the average LPC production for each treatment with S.E.M. of three experiments is shown; \*P < 0.05 M. (c) HUVECs were treated with various LPC species (up to 20 μM). Viability curves at 24 h after treatment with average percent of survival and S.E.M. from three experiments are shown. (d, e) HUVECs were treated with 10 μM of each indicated LPC species. Cells were lysed 5 min later and subjected to western blot analysis for phospho- and total ERK1/2 (c), phospho- and total Akt (d), and actin

this enhanced cell death, we first analyzed the effect of cPLA<sub>2</sub> inhibition on cell-cycle regulation in irradiated endothelial cells. As expected,<sup>20</sup> radiation alone caused a significant increase in the percentage of cells in G<sub>1</sub>/G<sub>0</sub> phase that was concurrent with a decrease in S phase at 24–48 h (data not shown). Similar results were observed in irradiated cells pretreated with cPLA<sub>2</sub> inhibitors (data not shown). We next studied levels of cyclin B1, which regulates activity of Cdk1 and transition through the cell cycle.<sup>21,22</sup> After 24–48 h of treatment, cyclin B1 was dramatically increased in the cells treated with cPLA<sub>2</sub> inhibitors and radiation, whereas cells

treated with radiation alone showed a significant delay in cyclin B1 expression (Figure 5e). As we did not detect any significant differences in cell cycle between irradiated cells and cells treated with cPLA<sub>2</sub> inhibitors and radiation, the observed cyclin B1 accumulation was cell cycle independent that can be associated with mitotic catastrophe.<sup>22–24</sup> Thus, we determined the effect of cPLA<sub>2</sub> inhibition on the morphology of irradiated endothelial cells after 24–96 h of treatment. At 24–48 h after combined treatment, we observed a sixfold increase in multinucleated giant cells compared to control cells (Figures 5c and d). This effect was

also detected in cells treated with radiation alone, but it was delayed and significantly less pronounced (Figure 5d). The formation of multinucleated giant cells concurrent with cell cycle-independent accumulation of cyclin B1 implicates mitotic catastrophe occurring during the inhibition of cPLA<sub>2</sub>-dependent pro-survival signaling in irradiated endothelial cells.

In most cases, mitotic catastrophe evolves to cell death through apoptosis.<sup>22,23</sup> To determine whether apoptosis occurred in irradiated HUVECs pretreated with cPLA<sub>2</sub> inhibitors, we studied Annexin V and propidium iodide (PI) staining as well as nuclear morphology using PI staining. In both assays, we did not detect an increase in programmed cell death at 24–48 h after treatment (Figures 5f–h). However, when HUVECs were pretreated with cPLA<sub>2</sub> inhibitors prior to irradiation, number of Annexin V-positive cells increased by

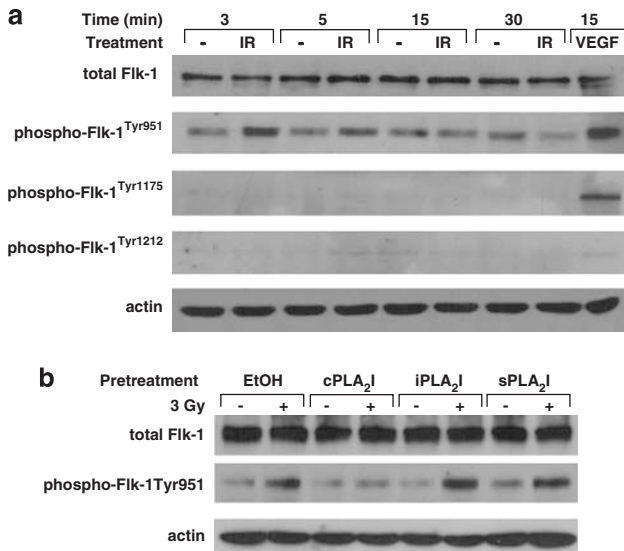


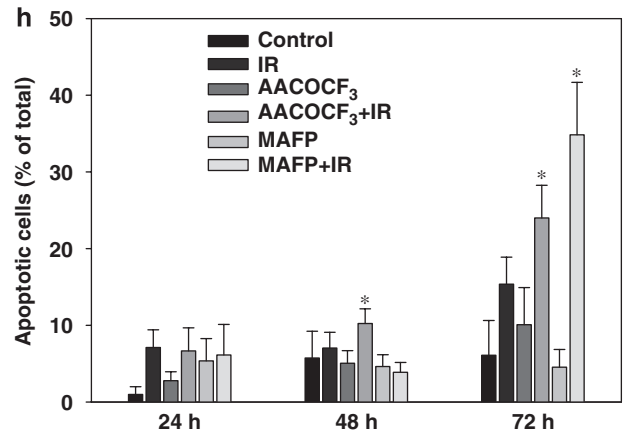
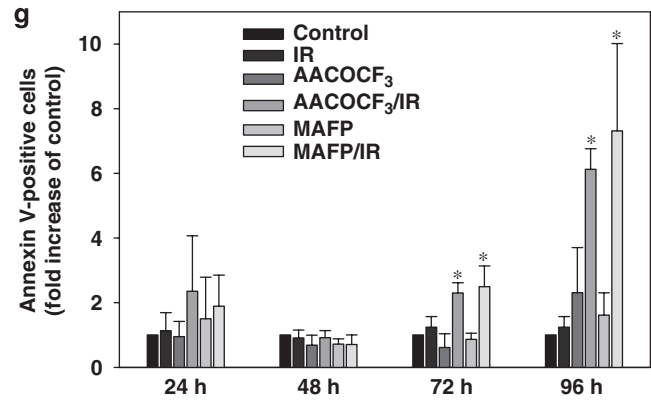
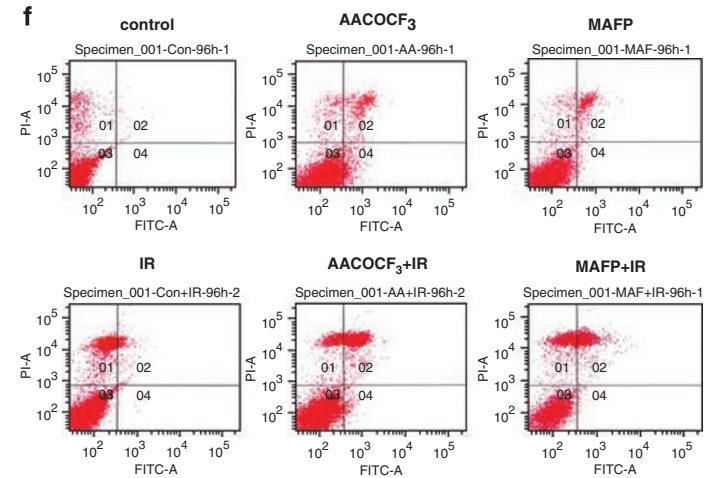
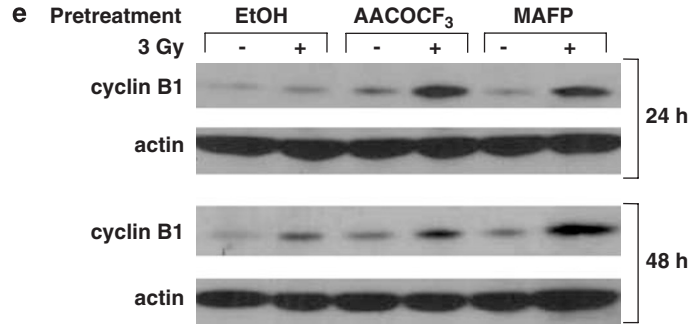
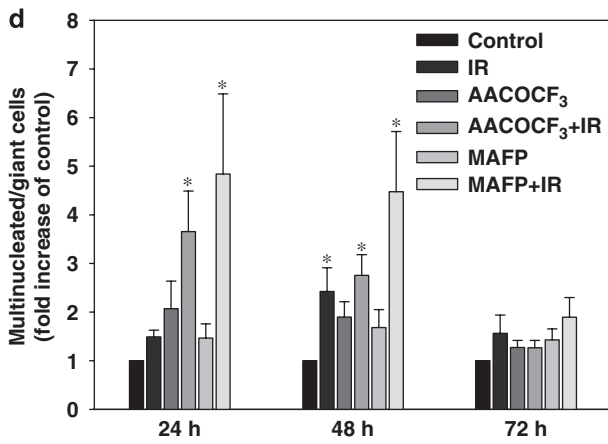
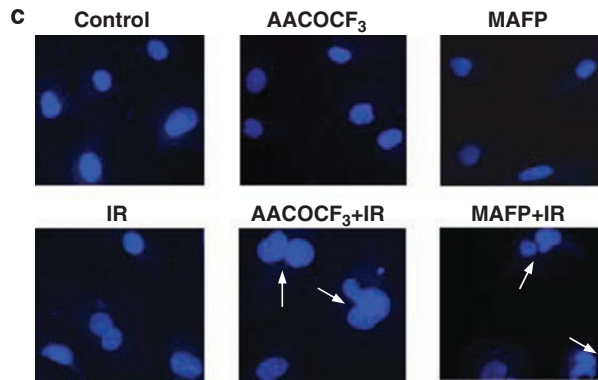
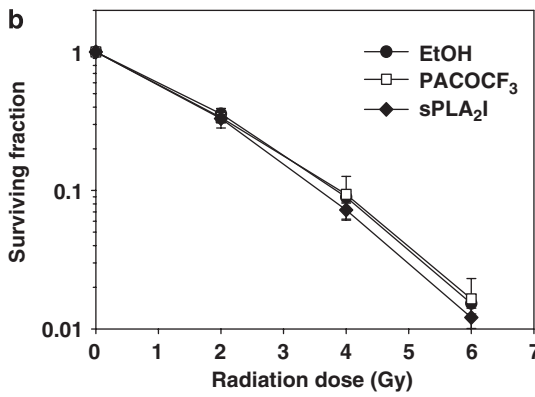
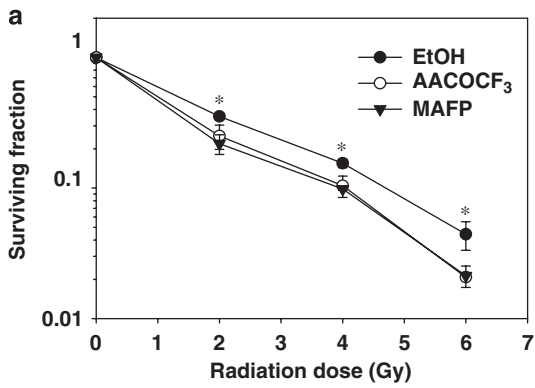
**Figure 4** Inhibition of cytosolic phospholipase A<sub>2</sub> (cPLA<sub>2</sub>) decreases radiation-induced phosphorylation of Flk-1. (a) Human umbilical vein endothelial cells (HUVECs) were treated with 3 Gy and lysed 3–30 min after the beginning of irradiation. Treatment with 100 ng/ml VEGF for 15 min was used as positive control. The western blot analysis with phospho-specific antibodies to Flk-1<sup>Tyr951</sup>, Flk-1<sup>Tyr1175</sup>, Flk-1<sup>Tyr1212</sup>, total Flk-1, and actin is shown. (b) HUVECs were treated with 3 Gy radiation or in combination with PLA<sub>2</sub> inhibitors as described in Figure 1d–f. Cells were lysed 3 min after the beginning of irradiation. The western blot for Flk-1<sup>Tyr951</sup>, total Flk-1, and actin is shown

2- to 3-fold at 72 h and by 7- to 11-fold at 96 h, compared to control cells (Figures 5f and g). Moreover, PI staining showed a 30–40% increase in apoptotic nuclei at 72 h after treatment (Figure 5h).

To verify the role of cPLA<sub>2</sub> in radiation-induced cell viability, we studied mitotic catastrophe and apoptosis in irradiated HUVECs transfected with nonsilencing shRNA or cPLA<sub>2</sub> shRNA as well as in irradiated MEF<sup>cPLA2x+/+</sup> and MEF<sup>cPLA2x-/-</sup>. Trends similar to the effects of cPLA<sub>2</sub> inhibitors in irradiated HUVECs were observed in both genetic models (Figure 6). In HUVECs transfected with cPLA<sub>2</sub> shRNA, the mitotic catastrophe at 48 h after irradiation was significantly increased compared to sham-irradiated cells (60 versus 40%; Figures 6a and b). This difference was sustained up to 96 h after radiation, whereas no statistically significant changes in mitotic catastrophe were observed in irradiated and sham-irradiated HUVECs transfected with nonsilencing shRNA over the course of the study (Figure 6b). In apoptotic experiments, 24, 48, or 72 h after irradiation, no significant change was observed in either cell type (Figure 6c). However, 96 h after treatment, irradiated HUVECs transfected with cPLA<sub>2</sub> shRNA but not with nonsilencing shRNA demonstrated modest but statistically significant increase in apoptosis, compared to sham-irradiated cells (60 versus 45%; Figure 6c). In irradiated MEF<sup>cPLA2x+/+</sup> and MEF<sup>cPLA2x-/-</sup>, similar levels of increase in the amount of multinucleated/giant cells were observed at 24 and 48 h after treatment compared to sham-irradiated cells (60 versus 30%; Figure 6d). At 72 h, this difference was sustained in irradiated MEF<sup>cPLA2x+/+</sup>, but not in MEF<sup>cPLA2x-/-</sup> (Figure 6d). In the apoptotic study, 24 or 48 h after irradiation, no significant change was observed in either cell type (Figure 6e). However, 72–96 h after treatment, irradiated MEF<sup>cPLA2x-/-</sup> demonstrated an increase in apoptosis up to fourfold, compared to sham-irradiated cells (80 versus 20%; Figure 6e). In contrast, we observed no statistically significant increase in apoptosis in irradiated MEF<sup>cPLA2x+/+</sup> versus control cells (Figure 6e).

**Effects of cPLA<sub>2</sub> on endothelial functions in irradiated HUVECs.** We investigated the role of cPLA<sub>2</sub> in HUVECs migration by using two approaches: endothelial cell migration through a filter and endothelial cell gash closure (Figure 7). In both assays, radiation alone or inhibition of cPLA<sub>2</sub> with AACOCF<sub>3</sub> alone resulted in a 15% decrease in HUVEC migration, which was not statistically significant (Figures 7a

**Figure 5** Inhibition of cytosolic phospholipase A<sub>2</sub> (cPLA<sub>2</sub>) decreases clonogenic survival of irradiated human umbilical vein endothelial cells (HUVECs) and leads to mitotic catastrophe within 24–48 h of irradiation followed by delayed programmed cell death at 72–96 h after irradiation. (a, b) HUVECs were plated on fibronectin-coated plates. Inhibitors for cPLA<sub>2</sub> (a) or intracellular Ca<sup>2+</sup>-independent (iPLA<sub>2</sub>) and secretory phospholipase A<sub>2</sub> (sPLA<sub>2</sub>) (b) were added 30 min before irradiation. After 2 weeks, colonies over 50 cells were counted and normalized for plating efficiency. Average surviving fractions and S.E.M. from three experiments are shown; \**P* < 0.05. (c, d) HUVECs were grown on slides, treated with EtOH or cPLA<sub>2</sub> inhibitors for 30 min, irradiated with 3 Gy, and fixed 24, 48 or 72 h later. Cells were stained with 4',6-diamidino-2-phenylindole (DAPI). (e) Microscopic photographs of DAPI-stained cells at 24 h after treatment are shown. Arrows indicate multinucleated/giant cells. (f) Multinucleated giant cells were counted in six randomly selected fields. A bar graph of the average fold increase in multinucleated/giant cells for each treatment compared to control cells with S.E.M. from four experiments is shown; \**P* < 0.05. (g) HUVECs were treated with EtOH (solvent control) or cPLA<sub>2</sub> inhibitors for 30 min, irradiated with 3 Gy and lysed after 24 or 48 h. The western blot analysis using anti-cyclin B1 and actin antibodies is shown. (h, g) HUVECs were treated with EtOH or cPLA<sub>2</sub> inhibitors for 30 min, irradiated with 3 Gy, collected after 24, 48, 72, and 96 h, stained with Annexin V-FITC and propidium iodide (PI), and analyzed by flow cytometry. (f) Representative diagrams of distribution of stained cells and (g) bar graph of the average fold increase in the percent apoptotic cells in each treatment normalized to control cells with S.E.M. of four experiments are shown; \**P* < 0.05. (h) HUVECs were grown on slides, treated with EtOH or cPLA<sub>2</sub> inhibitors for 30 min, irradiated with 3 Gy, fixed 24, 48, or 72 h later and stained with PI. Cells with chromatin condensation and nuclear fragmentation were counted in multiple randomly selected fields. A bar graph of the average percent of apoptotic cells for each treatment with S.E.M. from four experiments is shown; \**P* < 0.05



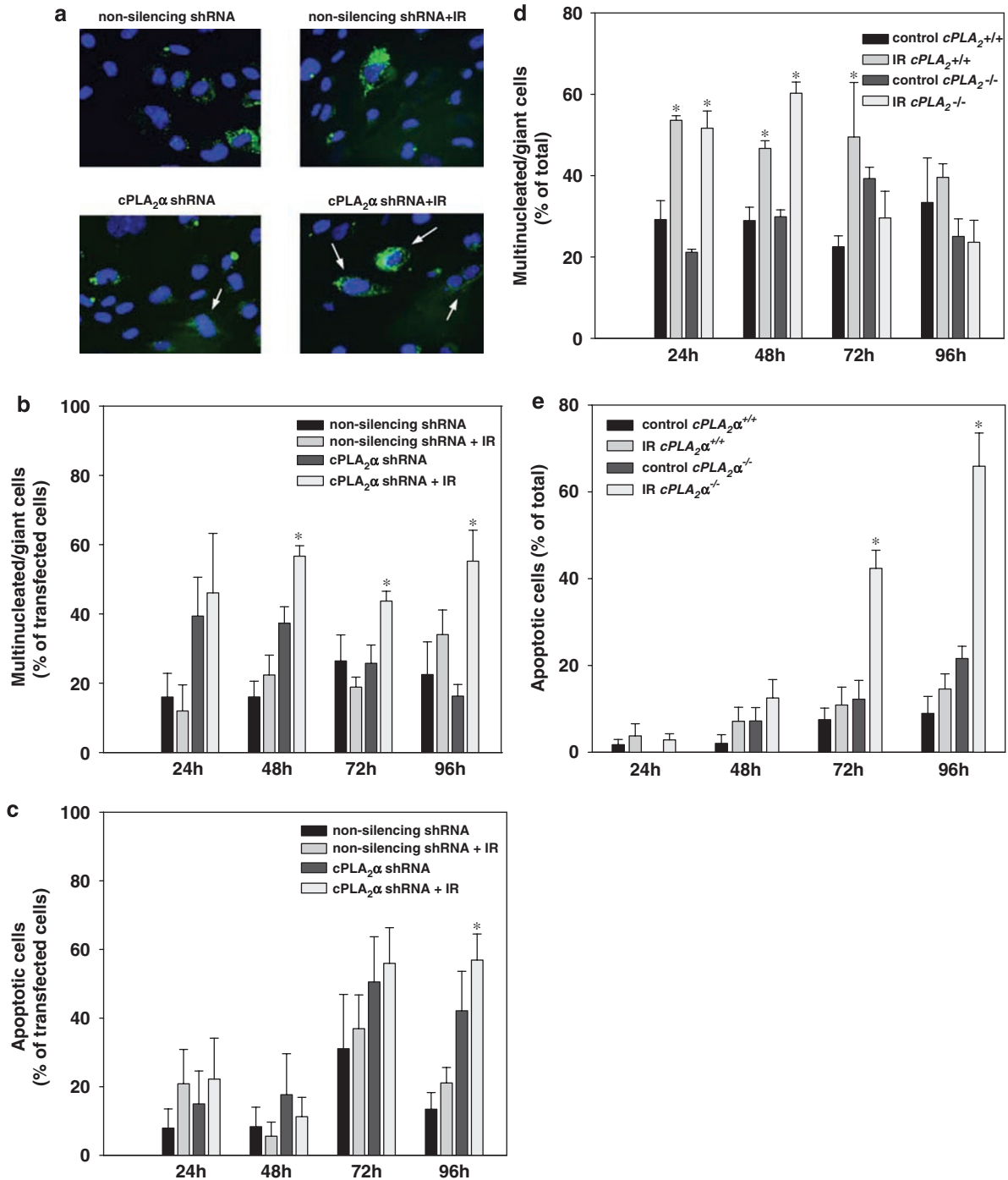


**Figure 6** Radiation leads to increase in multinucleated/giant and apoptotic cells following knockout or knockdown of cytosolic phospholipase A<sub>2</sub> (cPLA<sub>2</sub>) $\alpha$ . Human umbilical vein endothelial cells (HUVECs) transfected with nonsilencing shRNA or cPLA<sub>2</sub> $\alpha$  shRNA (a–c) and mouse embryonic fibroblasts cPLA<sub>2</sub> $\alpha$ <sup>+/+</sup> or cPLA<sub>2</sub> $\alpha$ <sup>-/-</sup> (d, e) were irradiated with 3 Gy and fixed 24, 48, 72, or 96 h later. Cells were stained with 4',6-diamidino-2-phenylindole (DAPI). (a) Microscopic photographs of DAPI-stained HUVECs 24 h after treatment are shown. GFP fluorescence (green) indicates transfected cells. Arrows indicate multinucleated/giant cells. (b, d) Multinucleated giant cells were counted in six randomly selected fields. Bar graphs of the average percent of multinucleated giant cells with S.E.M. from triplicates are shown; \**P* < 0.05. Transfected HUVECs (c) and fibroblasts (e) were grown on slides, irradiated with 3 Gy, fixed 24, 48, 72, or 96 h later and stained with propidium iodide. Cells with chromatin condensation and nuclear fragmentation were counted in six randomly selected fields. Bar graphs of the average percentage of apoptotic cells with S.E.M. from triplicates are shown; \**P* < 0.05

and c). Inhibition of cPLA<sub>2</sub> with MAFF alone demonstrated a greater decrease in gash closure than in migration through the filter (50 versus 20%; Figures 7a and c), possibly suggesting different mechanisms of cPLA<sub>2</sub> inhibition involved

in each type of migration. However, inhibition of cPLA<sub>2</sub> with either AACOCF<sub>3</sub> or MAFF followed by irradiation maximally abolished HUVEC migration in both assays leaving only 40% of cells capable of migration (Figure 7).



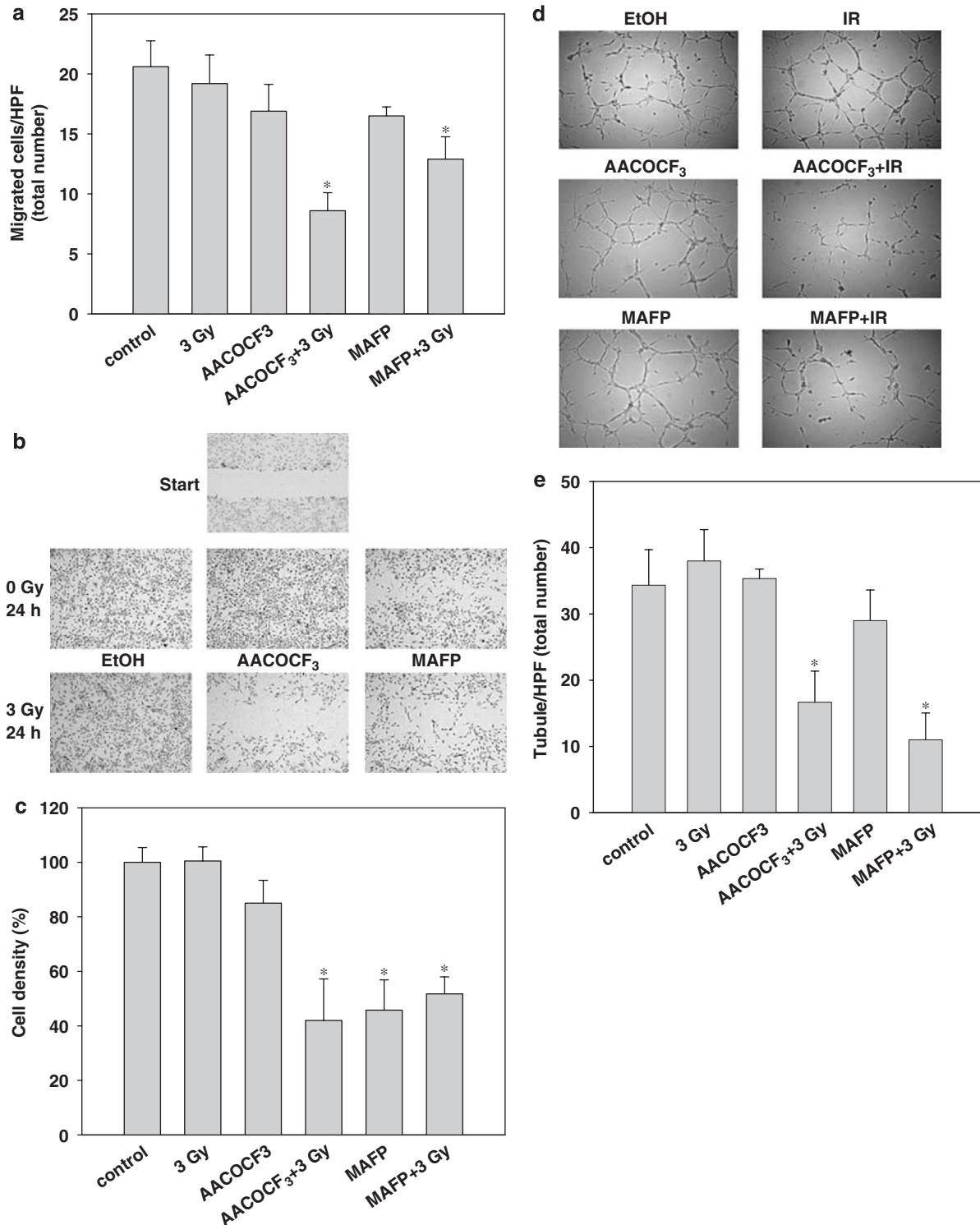


**Figure 7** Cytosolic phospholipase A<sub>2</sub> (cPLA<sub>2</sub>) inhibition decreases migration and tubule formation in irradiated human umbilical vein endothelial cells (HUVECs). (a) Endothelial cell migration assay. Fresh complete HUVEC medium was added to the bottom chamber of six-well plates with 8.0 μm inserts, whereas HUVEC suspension was added to the top chamber. Both chambers were treated with EtOH or cPLA<sub>2</sub> inhibitors for 30 min and irradiated with 3 Gy. After 24 h, cells in the insert chambers were stained with 4',6-diamidino-2-phenylindole (DAPI) and counted (five high-power fields (HPFs) per sample). The bar graph shows the mean and S.E.M. from six experiments for total number of migrated cells per HPF; \**P* < 0.05. (b, c) Endothelial cell gash closure assay. HUVECs were grown to 70–80% confluency. Four parallel wounds were created on each plate using a 200 μl pipette tip, and cells were treated with EtOH or cPLA<sub>2</sub> inhibitors for 30 min and irradiated with 3 Gy. After 24 h, cells were stained with 1% methylene blue and counted. (b) Micrographs of stained cells and (c) a bar graph of the corresponding average percentage of migrated cells with S.E.M. from six experiments are shown; \**P* < 0.05. (d, e) Capillary tubule formation assay. HUVECs were cultured onto Matrigel for 30 min, treated with EtOH or cPLA<sub>2</sub> inhibitors for 30 min, and irradiated with 3 Gy. Tubules were counted under microscopy 24 h later (five HPFs per sample). (d) Representative micrographs of capillary tubule formation and (e) total number of formed tubules per HPF in the bar graph with S.E.M. from six experiments are shown; \**P* < 0.05

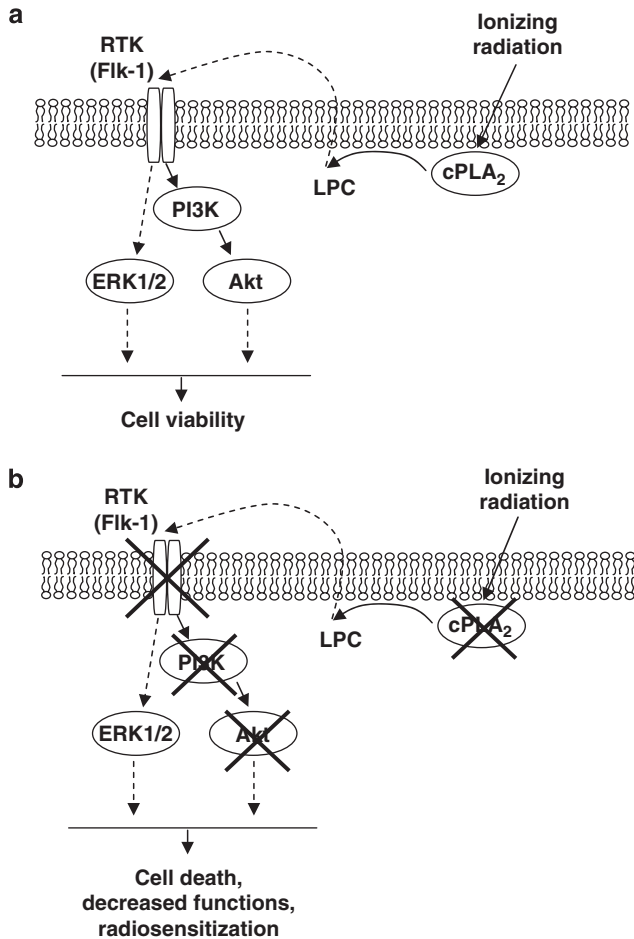


**Figure 8** Proposed sequence of molecular events in irradiated vascular endothelium. (a) Ionizing radiation triggers activation of cytosolic phospholipase A<sub>2</sub> (cPLA<sub>2</sub>) followed by increased production of lysophosphatidylcholine (LPC), activation of Flk-1 and phosphorylation of Akt and extracellular signal-regulated kinase (ERK)1/2 leading to cell viability. (b) Inhibition of this survival pathway at the level of various components (indicated by crosses) leads to cell death, decreased endothelial function, and increased radiosensitization

We also found that inhibition of cPLA<sub>2</sub> activity affected endothelial tubule formation in irradiated HUVECs. Untreated cells attached to matrigel when plated and formed capillary-like structures within 24 h following irradiation. Irradiated cells or cells treated with cPLA<sub>2</sub> inhibitors alone did not show significant difference in the number of capillary-like tubules compared to that of untreated cells (Figures 7d and e). However, irradiation combined with cPLA<sub>2</sub> inhibition caused a pronounced decrease of threefold (30% of control) in the number of formed tubules (Figures 7d and e).

## Discussion

Many common and life-threatening human diseases, including atherosclerosis, diabetes, cancer, and aging, have free radical reactions as an underlying mechanism of injury. Free radicals and other reactive oxygen and nitrogen species (ROS/RNS) are generated endogenously.<sup>25</sup> Overproduction of ROS results in oxidative stress, a deleterious process that can be an important mediator of damage to cell structures and

biological molecules. In contrast, beneficial effects of ROS occur at low/moderate concentrations and involve physiological roles in cellular responses, such as in the activation of signaling pathways.<sup>7,8,25</sup> ROS/RNS-dependent damage to vascular endothelium involving radiation-induced environmental stress and radiotherapy is widely studied.<sup>26,27</sup> However, the role of activation of pro-survival signal transduction pathways regulating the increased viability of vascular endothelial cells in response to low doses of ionizing radiation is underestimated and understudied.

**Immediate pro-survival signaling in irradiated vascular endothelial cells.** Our previous studies have shown that ionizing radiation triggers pro-survival signaling pathways that are specific and responsible for the inherent radioresistance of vascular endothelium.<sup>4–6,28</sup> However, the detailed mechanism of activation of these pathways is not known, especially immediate events. Here we demonstrated that 3 Gy of ionizing radiation induced phosphorylation of two pro-survival kinases Akt and ERK1/2 at 2 min with maximum occurring at 3 min after exposure. Rapid and transient activation of these kinases could involve interaction of radiation-triggered ROS with membrane lipids, signaling proteins, or DNA.<sup>1,29,30</sup> We were specifically interested in lipid-derived second messengers that are immediately mobilized following irradiation. One such signaling pathway involves PLA<sub>2</sub>. In irradiated HUVECs, we detected immediate activation of cytosolic PLA<sub>2</sub>. Moreover, radiation-induced phosphorylation of Akt and ERK1/2 was dependent on and occurred immediately after activation of cPLA<sub>2</sub>. Similar results were obtained using irradiated HUVECs transfected with shRNA for cPLA<sub>2</sub> $\alpha$  compared to nonsilencing shRNA and MEFs from wild-type and KO mice for cPLA<sub>2</sub> $\alpha$ , confirming a regulatory role of cPLA<sub>2</sub> in the activation of radiation-induced activation of ERK1/2 and Akt and suggesting that the  $\alpha$ -isoform of cPLA<sub>2</sub> family is a principal enzyme responsible for this regulation.

Activation of cPLA<sub>2</sub> leads to the increased production of lysophospholipids, such as LPC.<sup>12,14,31</sup> This biologically active lipid functions as the second messenger in signal transduction pathways, that regulate vascular proliferation, migration, expression of adhesion molecules, and inflammation.<sup>14–16</sup> In our study of irradiated HUVECs, LPC production was increased by 1.6-fold compared to untreated cells. To test whether this is involved in transduction of radiation signal, we compared HUVEC responses to ionizing radiation to the responses caused by exogenously added LPC. Cellular survival and proliferation in response to LPC treatment are dependent on LPC concentration.<sup>14</sup> Up to 25  $\mu$ M of LPC have been reported to increase proliferation of HUVECs,<sup>15</sup> whereas higher concentrations promoted cell death.<sup>32</sup> In our study, 10  $\mu$ M of four different exogenous LPC species did not cause a statistically significant change in cell proliferation. In addition, 10  $\mu$ M of various LPC species resulted in ERK1/2 and Akt phosphorylation similar to those observed in irradiated cells. This suggests that PLA<sub>2</sub>-dependent production of LPC could be the mediator of endothelial radioresistance. Similarly, Fujita *et al.*<sup>15</sup> have shown that 20  $\mu$ M LPC activated the same pro-survival kinases leading to increased HUVEC proliferation. The study also demonstrated

LPC-dependent transactivation of Flk-1 (VEGFR2/KDR-1) followed by activation of cSrc. Interestingly, radiation-induced Akt phosphorylation is inhibited by specific inhibitors of VEGFR2, PI3K/Akt, and cSrc.<sup>3,4,6,28,33</sup> The role of Flk-1 in the radiation response of vascular endothelium is widely studied,<sup>28,34</sup> however, the molecular mechanism of its radiation-induced activation is unknown. Upon ligand binding, Flk-1 undergoes autophosphorylation and becomes activated. Major autophosphorylation sites of Flk-1 are located in the kinase domain (Tyr<sup>951/996</sup>) and in the tyrosine kinase catalytic domain (Tyr<sup>1054/1059</sup>).<sup>35</sup> Here, we demonstrated that ionizing radiation resulted in specific phosphorylation of Flk-1 at Tyr<sup>951</sup> that was specifically abrogated by inhibition of cytosolic PLA<sub>2</sub>, but not Ca<sup>2+</sup>-independent or secretory members of PLA<sub>2</sub> family. Taken together with the study of Fujita *et al.*,<sup>15</sup> we speculate that in vascular endothelial cells radiation-induced production of LPC leads to transactivation of Flk-1.

**cPLA<sub>2</sub> in viability and inherent radioresistance of irradiated cells.** We also have shown that inhibition of cPLA<sub>2</sub> significantly enhanced radiation-induced cell death in endothelial cells. We characterized the mechanisms of this cell death and detected an increased number of multinucleated giant cells and cell cycle-independent accumulation of cyclin B1 within 24–48 h of irradiation. These features are characteristic of mitotic catastrophe.<sup>36</sup> Later, mitotic catastrophe led to a delayed programmed cell death, which was detected at 72–96 h after treatment. In addition to regulation of viability of endothelial cells, we demonstrated that cPLA<sub>2</sub> inhibition affected endothelial cell function, resulting in attenuated migration and tubule formation in irradiated HUVECs.

The role of cPLA<sub>2</sub> in pro-survival signaling, viability, and radioresistance of irradiated cells was also confirmed using genetic knockdown and KO models. However, although the shRNA approach using HUVECs resulted in effects very similar to those observed in irradiated HUVECs pretreated with chemical inhibitors of cPLA<sub>2</sub>, the effects in cPLA<sub>2</sub> KO MEFs were less pronounced. We anticipated an explanation for the difference in genetic manipulation of cPLA<sub>2</sub> (acutely decreased protein level in knockdown model *versus* KO model) that allows for compensation mechanisms when other isoforms of enzyme could take over the functions of knocked-out member of the family.

There are great differences in human organ and tissue sensitivity for radiation-induced damage.<sup>37,38</sup> Low doses of ionizing radiation (2–3 Gy) do not affect viability of vascular endothelial cells. Moreover, there are studies demonstrating that active cPLA<sub>2</sub> and its product LPC are necessary for viability and proliferation of endothelial cells.<sup>15,39</sup> We determined immediate radiation-dependent activation of a pro-survival signaling pathway that regulates viability and function of vascular endothelium. Our studies indicate a sequence of molecular events in irradiated endothelial cells, constituting an immediate signaling pathway activated by ionizing radiation (Figure 8a). Activation of cPLA<sub>2</sub> resulted in the production of LPC, transactivation of Flk-1, and subsequent phosphorylation of Akt and ERK1/2. Inhibition of this pathway at different levels<sup>3,5,6,28</sup> enhanced radiation-induced cell death

characterized by mitotic catastrophe followed by a delayed programmed cell death (Figure 8b). We propose that cPLA<sub>2</sub> signaling mediates radiation-dependent pro-survival response in vascular endothelial cells and, therefore, could represent one key regulator of inherent endothelial radioresistance. These data establish a biological basis for development of radiation mitigators and protectors.

## Materials and Methods

**Chemicals.** Organic solvents and PLA<sub>2</sub> inhibitors (AACOCF<sub>3</sub> and MAFF, cytosolic cPLA<sub>2</sub> inhibitors; PACOCF<sub>3</sub>, Ca<sup>2+</sup>-independent PLA<sub>2</sub> inhibitor; cyclic (2-naphthyl)Ala-Leu-Ser-2-naphthyl)Ala-Arg, secreted sPLA<sub>2</sub>-IIA inhibitor I) were purchased from EMD Biosciences (San Diego, CA, USA). Tridecanoyl LPC (13:0), palmitoyl LPC (16:0); stearoyl LPC (18:0); oleoyl LPC (18:1); arachidoyl LPC (20:0); phosphatidylcholine (PC); phosphatidic acid (PA); lysophosphatidic acid (LPA), and sphingomyelin (SM) were purchased from Avanti Polar Lipids (Alabaster, AL, USA). All other chemicals were purchased from Sigma (St. Louis, MO, USA).

**Cell culture and treatment.** Primary culture of HUVECs pooled from multiple donors was obtained from Cambrex (East Rutherford, NJ, USA) and was maintained in EBM-2 medium (Cambrex). Embryonic fibroblasts from cPLA<sub>2</sub> $\alpha^{-/-}$  and cPLA<sub>2</sub> $\alpha^{+/+}$  mice (MEF<sup>cPLA<sub>2</sub> $\alpha^{-/-}$</sup>  and MEF<sup>cPLA<sub>2</sub> $\alpha^{+/+}$</sup> ) were kindly provided by Dr. JV Bonventre (Renal Unit, Brigham Women's Hospital, Harvard Medical School, Boston, MA, USA). MEFs were maintained in Dulbecco's modified Eagle's medium/F-12 (1/1) with 10% FBS and 1% penicillin/streptomycin (Life Technologies, Gaithersburg, MD, USA). Cells from passages 2–5 were used in this study. HUVECs were starved for 6 h before treatment in MCDB 131 medium (Invitrogen, Carlsbad, CA, USA) supplemented with 0.2% BSA. For the irradiation of cells, Therapax DXT 300 X-ray machine (Pantak Inc., East Haven, CT, USA) delivering 2.04 Gy/min at 80 kVP or Mark I <sup>137</sup>Cs irradiator (JL Shepherd and Associates, San Fernando, CA, USA) delivering 1.84 Gy/min were used. Due to high sensitivity of HUVECs to temperature and pH, cells were carried to the irradiator and back to the incubator in gas/temperature-controlled chamber (5% CO<sub>2</sub>, 37°). In experiments with PLA<sub>2</sub> inhibitors, cells were treated for 30 min prior to 3 Gy irradiation with either 70% EtOH (control) or 1  $\mu$ M AACOCF<sub>3</sub>, 1  $\mu$ M MAFF, 1  $\mu$ M PACOCF<sub>3</sub>, and 100 nM sPLA<sub>2</sub>-IIA inhibitor I dissolved in 70% EtOH. In experiments with LPC, cells were treated with either 70% EtOH (control) or with different species of LPC (10–80  $\mu$ M) dissolved in 70% EtOH.

**shRNA silencing of cPLA<sub>2</sub> $\alpha$ .** HUVECs were transiently transfected using the pGIPZ lentiviral plasmid vector (Open Biosystems, Huntsville, AL, USA). This bicistronic vector allows estimation of the level of transfection by the expression of shRNA of interest in the first cistron, while keeping a high level of expression from second cistron encoding GFP. The vector contained either nonsilencing shRNA or shRNA for human cPLA<sub>2</sub> $\alpha$  (forward strand: CCTGTATTCTCACCCTGATT; reversed strand: AATCAGGGTGAGAATACAAGGT). Quality control of the vectors was performed by restriction enzyme digestion with *Sa*I. Once HUVECs reached 50% confluency, cells were transfected with 5  $\mu$ g of shRNA plasmid DNA in serum-free medium. After 48 h of incubation, the medium was aspirated and cells were replenished with endothelial growth medium. Cells were then examined microscopically for TurboGFP expression to estimate the level of transfection and then subjected to further treatment.

**Immunoblot analysis.** After treatment, HUVECs or MEFs were harvested at the indicated times. Total protein extraction was performed using M-PER kit (Pierce, Rockford, IL, USA). Protein concentration was quantified using BCA Reagent (Pierce). Protein extracts (40  $\mu$ g) were subjected to western immunoblot analysis using antibodies for the detection of phospho-Akt<sup>Thr308/Ser473</sup>, phospho-ERK1/2<sup>Thr202/Tyr204</sup>, phospho-Flk-1<sup>Tyr951</sup>, phospho-Flk-1<sup>Tyr1175</sup>, phospho-Flk-1<sup>Tyr1212</sup>, total Akt, ERK1/2, and Flk-1, and cyclin B1 (all from Cell Signaling Technologies, Danvers, MA, USA). Antibody to actin (Sigma) was used to evaluate protein loading in each lane. Immunoblots were developed using the Western Lightning Chemiluminescence Plus detection system (PerkinElmer, Wellesley, MA, USA) according to the manufacturer's protocol.

**PLA<sub>2</sub> activity.** After treatment, HUVECs were harvested and assayed for PLA<sub>2</sub> activity using PLA<sub>2</sub> activity kit (Cayman, Ann Arbor, MI, USA) according to manufacturer's instructions. Briefly, 1.5 mM arachidonoyl thio-phosphotidylcholine (PLA<sub>2</sub> substrate) was incubated with 20  $\mu$ l of lysed cells in 96-well plate for 1 h at room temperature. Reaction was stopped by addition of DTNB/EGTA, and optical density (OD) was measured using Microplate reader at 405 nm. Average fold increase in PLA<sub>2</sub> activity was calculated as (OD of treated samples normalized to sample total protein)/(OD of control normalized to control total protein) with S.E.M. from three experiments.

**Clonogenic survival.** HUVECs were plated on fibronectin-lined plates (BD Biosciences, Bedford, MA, USA) and were allowed to attach for 5 h. Cells were then treated with EtOH or various PLA<sub>2</sub> inhibitors followed by irradiation with 0, 2, 4, or 6 Gy. Medium was changed after irradiation. After 10–14 days, plates were fixed with 70% EtOH and stained with 1% methylene blue. Colonies consisting of over 50 cells were counted with a dissection microscope. Average survival fraction was calculated as (number of colonies/number of cells plated)/(number of colonies for corresponding control/number of cells plated) with S.E.M. from three experiments.

**Morphologic analysis of cells stained with DAPI or PI.** HUVECs were grown on slides, treated with EtOH or cPLA<sub>2</sub> inhibitors for 30 min and irradiated with 3 Gy. In shRNA approach, HUVECs were grown on slides, transfected with nonsilencing shRNA or cPLA<sub>2</sub> $\alpha$  shRNA and irradiated with 3 Gy 48 h later. MEF<sup>cPLA2 $\alpha$ -/-</sup> and MEF<sup>cPLA2 $\alpha$ +/+</sup> were grown on slides and irradiated with 3 Gy. After 24, 48, 72, and 96 h post-irradiation, cells were fixed in 100% cold methanol. Cells were stained with 2.5  $\mu$ g/ml 4',6-diamidino-2-phenylindole (DAPI) in phosphate-buffered saline (PBS) (Life Technologies) or with 1.0  $\mu$ g/ml PI in PBS. During the shRNA approach, transfected HUVECs were fixed in 4% paraformaldehyde to retain high level of GFP fluorescence and treated with 100  $\mu$ g/ml RNase for 30 min at 37°C to prevent RNA staining by PI. Photographs were taken using an Olympus BX60 fluorescent microscope equipped with Retiga 2000R digital camera. Images were processed using AxioVision Software. Giant multinucleated cells (for HUVECs) and cells with nuclear condensation and fragmentation (for HUVECs and MEFs) were counted in multiple randomly selected fields. The average percentage of such cells over total cell number or average fold increase over control was calculated with S.E.M. from four experiments.

**Flow cytometry analysis with annexin V-FITC and PI.** Treated HUVECs were collected after 24, 48, 72, and 96 h. Annexin V-FITC apoptosis Detection Kit (BD Pharmingen, San Diego, CA, USA) was used for staining of the cells. Briefly, Annexin V-FITC (5 ng) and PI (50 ng) were added to 10<sup>5</sup> cells. Stained cells were analyzed by flow cytometry. For each treatment, the average fold increase of apoptotic cells over control ( $\pm$  S.E.M. from four experiments) was calculated.

**Thin-layer chromatography for LPC detection.** HUVECs were grown to 90% confluency in 100 mm culture dishes, washed twice with PBS, and labeled for 90 min using <sup>3</sup>H-palmitic acid (10  $\mu$ Ci/ml in PBS, pH 7.5) (Perkin Elmer Welleley, MA, USA). After labeling, cells were washed twice with PBS, treated with 3 Gy, and placed on ice 3 min after the beginning of irradiation. Lipids were extracted using a modified Bligh and Dyer method.<sup>40</sup> Briefly, cells were scraped in 0.8 ml of cold acidified MeOH (0.1 M HCl:methanol, 1 : 1, v/v), transferred into cold 1.5 ml tubes, and vortexed for 1 min with 0.4 ml cold chloroform. The extractions were centrifuged at 18 000  $\times$  g for 5 min at 4°C, dried, and dissolved in 20  $\mu$ l of chloroform. The samples were spotted onto 0.25 mm Silica Gel 60 Å TLC plate (Whatman Inc., Florham Park, NJ, USA) along with standards (PC, LPC, PA, LPA, and SM), resolved with chloroform:methanol:acetic acid:water (50 : 28 : 4 : 8 by volume) and stained with iodine vapor. The TLC plate was then dried and exposed to a Phosphorimager tritium screen (GE Healthcare, Piscataway, NJ, USA) for 90 h. The average amount of labeled LPC ( $\pm$  S.E.M. from three experiments) was quantitated using Typhoon 9400 Variable mode Imager (GE Healthcare).

**Cell proliferation assay.** HUVECs were plated into a 96-well plate at a density of 5  $\times$  10<sup>3</sup> cells per well. The following day cells were treated with varying concentrations of different LPC species (16 : 0, 18 : 0, 18 : 1, or 20 : 0) dissolved in 70% EtOH. After 24 h of treatment, 10  $\mu$ l of WST-1 reagent from Rapid Cell Proliferation Kit (EMD Biosciences) were added to each well, followed by 1 h incubation at 37°C. OD was measured using Microplate reader at 460 nm. Average

cell survival ( $\pm$  S.E.M. from three experiments) was calculated as a percent of untreated.

**Endothelial cell migration assays.** To estimate HUVEC migration through the filter, fresh complete HUVEC medium was added to the bottom chamber of six-well plates with 8.0  $\mu$ M inserts (BD Biosciences, Bedford, MA, USA), whereas HUVEC suspension (2.5  $\times$  10<sup>4</sup> cells per ml in starvation medium) was added to the top chamber. Cells were allowed to attach for 30 min and both chambers were treated with cPLA<sub>2</sub> inhibitors (1  $\mu$ M AACOCF<sub>3</sub> and 1  $\mu$ M MAFF) for 30 min followed by 3 Gy radiation. After 24 h the top layer of cells (nonmigrated cells) were removed with a cotton swab. The insert chambers were washed with PBS, fixed in MeOH, and stained with DAPI. Cells in five high-power fields (HPFs) from each sample were counted. The average number of migrated cells per HPF ( $\pm$  S.E.M. from six experiments) was calculated.

For the endothelial cell closure assay, HUVECs were grown to 70–80% confluency. Four parallel wounds were created on each plate using a 200  $\mu$ l pipette tip, and cells were treated with cPLA<sub>2</sub> inhibitors (1  $\mu$ M AACOCF<sub>3</sub> and 1  $\mu$ M MAFF) for 30 min followed by 3 Gy radiation. After 24 h cells were stained with 1% methylene blue and five HPFs from each sample were counted. The average percent of cell density in the wounded area for each treatment was calculated as (number of cells in wounded area)/(number of cells in unwounded area) with S.E.M. from six experiments.

**Tubule formation in matrigel.** Matrigel (75  $\mu$ l per well; BD Biosciences) was added to a 96-well plate and allowed to solidify at 37°C. HUVECs (10  $\times$  10<sup>3</sup> cells per well) were plated onto Matrigel. 30 min later cPLA<sub>2</sub> inhibitors (1  $\mu$ M AACOCF<sub>3</sub> and 1  $\mu$ M MAFF) were added followed by irradiation with 3 Gy 30 min later. Once capillary-like tubules were formed from the control cells (2–6 h), digital microphotographs of the wells were taken. Average number of tubules was quantified from the photographs with S.E.M. from six experiments.

**Statistical analysis.** The mean and S.E.M. of each treatment group were calculated. Variance was analyzed by Student's *t*-test; *P*-value < 0.05 was considered statistically significant.

**Acknowledgements.** We appreciate gift of mouse embryonic fibroblasts MEF<sup>cPLA2 $\alpha$ -/-</sup> and MEF<sup>cPLA2 $\alpha$ +/+</sup> from Dr. JV Bonventre (Harvard Medical School, Boston, MA, USA). This work was supported in part by NIH grants R01-CA112385, R01-CA88076, R01-CA89674, R01-CA89888, and P50-CA90949, Elsa U. Pardee Foundation, Ingram Charitable Fund and Vanderbilt-Ingram Cancer Center, CCSG P30-CA68485.

- Kolesnick R, Fuks Z. Radiation and ceramide-induced apoptosis. *Oncogene* 2003; **22**: 5897–5906.
- Haimovitz-Friedman A, Kan CC, Ehleiter D, Persaud RS, McLoughlin M, Fuks Z et al. Ionizing radiation acts on cellular membranes to generate ceramide and initiate apoptosis. *J Exp Med* 1994; **180**: 525–535.
- Geng L, Tan J, Himmelfarb E, Schueneman A, Niermann K, Brousal J et al. A specific antagonist of the p110delta catalytic component of phosphatidylinositol 3'-kinase, IC486068, enhances radiation-induced tumor vascular destruction. *Cancer Res* 2004; **64**: 4893–4899.
- Edwards E, Geng L, Tan J, Onishko H, Donnelly E, Hallahan DE. Phosphatidylinositol 3-kinase/Akt signaling in the response of vascular endothelium to ionizing radiation. *Cancer Res* 2002; **62**: 4671–4677.
- Tan J, Hallahan DE. Growth factor-independent activation of protein kinase B contributes to the inherent resistance of vascular endothelium to radiation-induced apoptotic response. *Cancer Res* 2003; **63**: 7663–7667.
- Tan J, Geng L, Yazlovitskaya EM, Hallahan DE. Protein kinase B/Akt-dependent phosphorylation of glycogen synthase kinase-3 $\beta$  in irradiated vascular endothelium. *Cancer Res* 2006; **66**: 2320–2327.
- Valerie K, Yacoub A, Hagan MP, Curiel DT, Fisher PB, Grant S et al. Radiation-induced cell signaling: inside-out and outside-in. *Mol Cancer Ther* 2007; **6**: 789–801.
- Mikkelsen RB, Wardman P. Biological chemistry of reactive oxygen and nitrogen and radiation-induced signal transduction mechanisms. *Oncogene* 2003; **22**: 5734–5754.
- MacLachlan T, Narayanan B, Gerlach VL, Smithson G, Gerwien RW, Folkerts O et al. Human fibroblast growth factor 20 (FGF-20; CG53135-05): a novel cytoprotectant with radioprotective potential. *Int J Radiat Biol* 2005; **81**: 567–579.
- Cabral GA. Lipids as bioeffectors in the immune system. *Life Sci* 2005; **77**: 1699–1710.
- Farooqui AA, Horrocks LA. Phospholipase A2-generated lipid mediators in the brain: the good, the bad, and the ugly. *Neuroscientist* 2006; **12**: 245–260.

12. Chakraborti S. Phospholipase A(2) isoforms: a perspective. *Cell Signal* 2003; **15**: 637–665.
13. Bonventre JV. The 85-kD cytosolic phospholipase A2 knockout mouse: a new tool for physiology and cell biology. *J Am Soc Nephrol* 1999; **10**: 404–412.
14. Prokazova NV, Zvezdina ND, Korotaeva AA. Effect of lysophosphatidylcholine on transmembrane signal transduction. *Biochemistry (Mosc)* 1998; **63**: 31–37.
15. Fujita Y, Yoshizumi M, Izawa Y, Ali N, Ohnishi H, Kanematsu Y *et al*. Transactivation of fetal liver kinase-1/kinase-insert domain-containing receptor by lysophosphatidylcholine induces vascular endothelial cell proliferation. *Endocrinology* 2006; **147**: 1377–1385.
16. Murugesan G, Sandhya Rani MR, Gerber CE, Mukhopadhyay C, Ransohoff RM, Chisolm GM *et al*. Lysophosphatidylcholine regulates human microvascular endothelial cell expression of chemokines. *J Mol Cell Cardiol* 2003; **35**: 1375–1384.
17. Sugiyama S, Kugiyama K, Ogata N, Doi H, Ota Y, Ohgushi M *et al*. Biphasic regulation of transcription factor nuclear factor-kappaB activity in human endothelial cells by lysophosphatidylcholine through protein kinase C-mediated pathway. *Arterioscler Thromb Vasc Biol* 1998; **18**: 568–576.
18. Dent P, Yacoub A, Fisher PB, Hagan MP, Grant S. MAPK pathways in radiation responses. *Oncogene* 2003; **22**: 5885–5896.
19. Dent P, Yacoub A, Contessa J, Caron R, Amorino G, Valerie K *et al*. Stress and radiation-induced activation of multiple intracellular signaling pathways. *Radiat Res* 2003; **159**: 283–300.
20. Hwang A, Muschel RJ. Radiation and the G<sub>2</sub> phase of the cell cycle. *Radiat Res* 1998; **150**: S52–S59.
21. Kramer A, Lukas J, Bartek J. Checking out the centrosome. *Cell Cycle* 2004; **3**: 1390–1393.
22. Castedo M, Perfettini JL, Roumier T, Kroemer G. Cyclin-dependent kinase-1: linking apoptosis to cell cycle and mitotic catastrophe. *Cell Death Differ* 2002; **9**: 1287–1293.
23. Castedo M, Perfettini JL, Roumier T, Andreau K, Medema R, Kroemer G. Cell death by mitotic catastrophe: a molecular definition. *Oncogene* 2004; **23**: 2825–2837.
24. Ianzini F, Bertoldo A, Kosmacek EA, Phillips SL, Mackey MA. Lack of p53 function promotes radiation-induced mitotic catastrophe in mouse embryonic fibroblast cells. *Cancer Cell Int* 2006; **6**: 11.
25. Valko M, Leibfriz D, Moncol J, Cronin MT, Mazur M, Telser J. Free radicals and antioxidants in normal physiological functions and human disease. *Int J Biochem Cell Biol* 2007; **39**: 44–84.
26. Rodel F, Keilholz L, Herrmann M, Sauer R, Hildebrandt G. Radiobiological mechanisms in inflammatory diseases of low-dose radiation therapy. *Int J Radiat Biol* 2007; **83**: 357–366.
27. Pelevina II, Gotlib V, Konradov AA. 20 years after Chernobyl accident – is it a lot or not for the estimation its characteristics? *Radiats Biol Radioecol* 2006; **46**: 240–247.
28. Geng L, Donnelly E, McMahon G, Lin PC, Sierra-Rivera E, Oshinka H *et al*. Inhibition of vascular endothelial growth factor receptor signaling leads to reversal of tumor resistance to radiotherapy. *Cancer Res* 2001; **61**: 2413–2419.
29. Kufe D, Weichselbaum R. Radiation therapy: activation for gene transcription and the development of genetic radiotherapy-therapeutic strategies in oncology. *Cancer Biol Ther* 2003; **2**: 326–329.
30. Truman JP, Gueven N, Lavin M, Leibel S, Kolesnick R, Fuks Z *et al*. Down-regulation of ATM protein sensitizes human prostate cancer cells to radiation-induced apoptosis. *J Biol Chem* 2005; **280**: 23262–23272.
31. Hirabayashi T, Murayama T, Shimizu T. Regulatory mechanism and physiological role of cytosolic phospholipase A2. *Biol Pharm Bull* 2004; **27**: 1168–1173.
32. Tsutsumi H, Kumagai T, Naitoo S, Ebina K, Yokota K. Synthetic peptide (P-21) derived from Asp-hemolysin inhibits the induction of apoptosis on HUVECs by lysophosphatidylcholine. *Biol Pharm Bull* 2006; **29**: 907–910.
33. Cuneo KC, Geng L, Tan J, Brousal J, Shinohara ET, Osusky K *et al*. SRC family kinase inhibitor SU6656 enhances antiangiogenic effect of irradiation. *Int J Radiat Oncol Biol Phys* 2006; **64**: 1197–1203.
34. Abdollahi A, Lipson KE, Han X, Krempien R, Trinh T, Weber KJ *et al*. SU5416 and SU6668 attenuate the angiogenic effects of radiation-induced tumor cell growth factor production and amplify the direct anti-endothelial action of radiation *in vitro*. *Cancer Res* 2003; **63**: 3755–3763.
35. Zaher TE, Miller EJ, Morrow DM, Javdan M, Mantell LL. Hyperoxia-induced signal transduction pathways in pulmonary epithelial cells. *Free Radic Biol Med* 2007; **42**: 897–908.
36. Ricci MS, Zong WX. Chemotherapeutic approaches for targeting cell death pathways. *Oncologist* 2006; **11**: 342–357.
37. Upton AC. Carcinogenic effects of low-level ionizing radiation. *J Natl Cancer Inst* 1990; **82**: 448–449.
38. Pierce DA, Shimizu Y, Preston DL, Vaeth M, Mabuchi K. Studies of the mortality of atomic bomb survivors. Report 12, Part I. Cancer: 1950–1990. *Radiat Res* 1996; **146**: 1–27.
39. Herbert SP, Ponnambalam S, Walker JH. Cytosolic phospholipase A2-alpha mediates endothelial cell proliferation and is inactivated by association with the Golgi apparatus. *Mol Biol Cell* 2005; **16**: 3800–3809.
40. Bligh EG, Dyer WJ. A rapid method of total lipid extraction and purification. *Can J Biochem Physiol* 1959; **37**: 911–917.